

High-resolution grid of H/V spectral ratios and spatial variability on microtremors at Port of Spain, Trinidad

Walter Salazar · Garth Mannette · Kafele Reddock · Clevon Ash

Received: 19 July 2016 / Accepted: 10 July 2017
© Springer Science+Business Media B.V. 2017

Abstract We performed dense single mobile microtremor measurements at 1181 sites throughout the city of Port of Spain, Trinidad. The results yielded fundamental periods of the soil of 1.2–1.7 s in the coastal areas, 0.3–1.2 s in the downtown area, and 0.0–0.3 s in the surrounding areas of the city. We employed the variogram plot to retrieve the spatial variability of fundamental periods. The results suggest that the variability of the period yields about 0.010 s^2 at short distances of 100 m and it can be modeled as a Gaussian distribution which is directionally dependent. Finally, we propose an elastic design response spectra for different zones in the city in accordance with the observed

periods of vibration and compatible with the International Building Code (IBC) provisions.

Keywords Spectral ratios · Fundamental period of soil · Variogram · Response spectrum

1 Introduction

The Trinidad and Tobago Microzonation Project is a 10-year project funded by the Ministry of Planning and Sustainable Development in collaboration with The University of the West Indies, Seismic Research Centre that started in 2013. This project seeks to assess the dynamic response characteristics of the ground under 10 towns and cities employing microtremors as the principal tool, throughout Trinidad and Tobago. The first city investigated was Port of Spain (POS), which is the capital of Trinidad and Tobago (Fig. 1a, b). Port of Spain has become one of the leading cities in the Caribbean, and it is a major center for commerce and administration for the country and the Caribbean as well as being a major shipping hub in the region. It is essential, therefore, that the level of seismic hazard is properly understood to allow adequate measures to mitigate risk, that caters for the production of maps that detail the different levels of a specified geotechnical hazard that may be triggered by an earthquake.

Destructive earthquakes worldwide have shown that local site effects have major effects on the ground shaking intensity as a phenomenon closely related to the filtering effects of the soil profile (Salazar et al. 2007;

W. Salazar (✉)
Faculty of Engineering and Architecture, Catholic University of El Salvador (UNICAES), Santa Ana, El Salvador
e-mail: walter.salazar@catolica.edu.sv
e-mail: walter.salazar.guerra@gmail.com

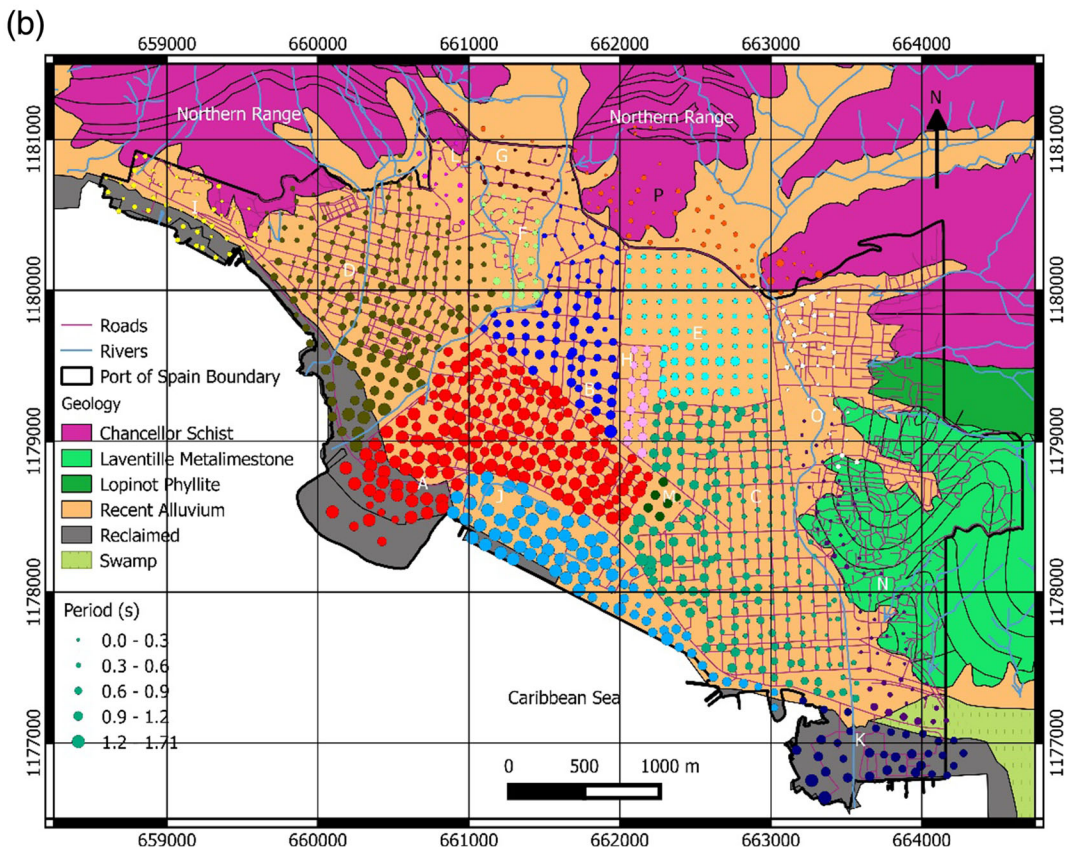
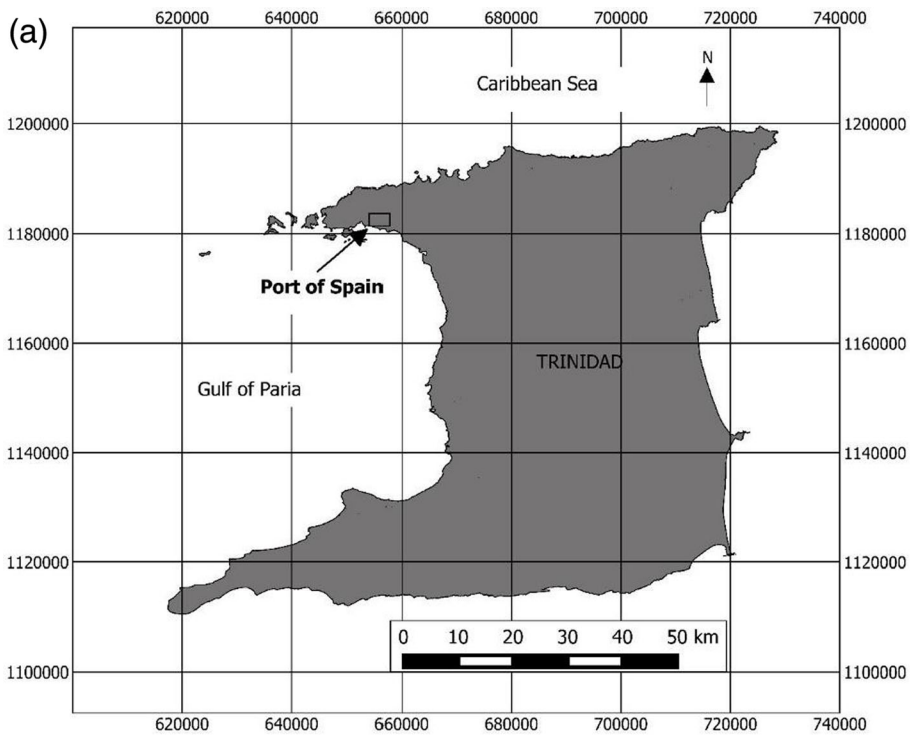
G. Mannette · K. Reddock · C. Ash
Seismic Research Centre, The University of the West Indies (UWI), St. Augustine, Trinidad and Tobago
e-mail: garth.mannette@sta.uwi.edu

G. Mannette
e-mail: gamannette@gmail.com

G. Mannette
e-mail: garth.mannete@gmail.com

K. Reddock
e-mail: hashimreddock@gmail.com

C. Ash
e-mail: cleveon.ash@uwiseismic.com



◀ **Fig. 1** **a** General location map of Trinidad and Port of Spain in the Eastern Caribbean. **b** Predominant period of vibration for soil deposits based on horizontal to vertical spectral ratio (H/V) employing the 1181 points of microtremor measurements in Port of Spain with an average of 85 m spacing. The units of the fundamental period of soil vibration are in seconds. The location of each microtremor measurement in each area (A–P) is depicted by *different color circles*. The 16 areas defined to perform the mobile microtremor survey are as follows: *A* Woodbrook, *B* St. Clair, *C* Port of Spain Proper, *D* St. James, *E* Queen’s Park Savannah, *F* Federation Park, *G* Ellerslie Park, *H* Newtown, *I* Cocorite, *J* port of Port of Spain, *K* Sea Lots, *L* Long Circular Road, *M* La Perouse Cemetery, *N* East Port of Spain, *O* Belmont, *P* peripheries

Salazar and Seo 2003). Several studies have shown that Nakamura’s technique (Nakamura 1989) for estimating shear wave resonant periods is a robust method that can yield useful information regarding the soil profile of a site in the near surface. In this work, we study the site effects in the city of POS in Trinidad by performing single mobile microtremor measurements at 1181 sites with the objective of computing the H/V spectral ratios.

We divide this article into five sections; firstly, we explain the geological setting of Port of Spain; secondly, the authors present the results of a high-resolution survey of mobile microtremors in POS in terms of the fundamental shear wave period of vibration of the soil deposits applying the method of H/V spectral ratios. Thirdly, we investigate the spatial variability of the data via application of a variogram plot; fourthly, we propose an elastic design response spectra of 5% damping for different zones of POS. Finally, we conclude our study with further recommendations for planning and research for the city of Port of Spain.

2 Geological setting of the Port of Spain

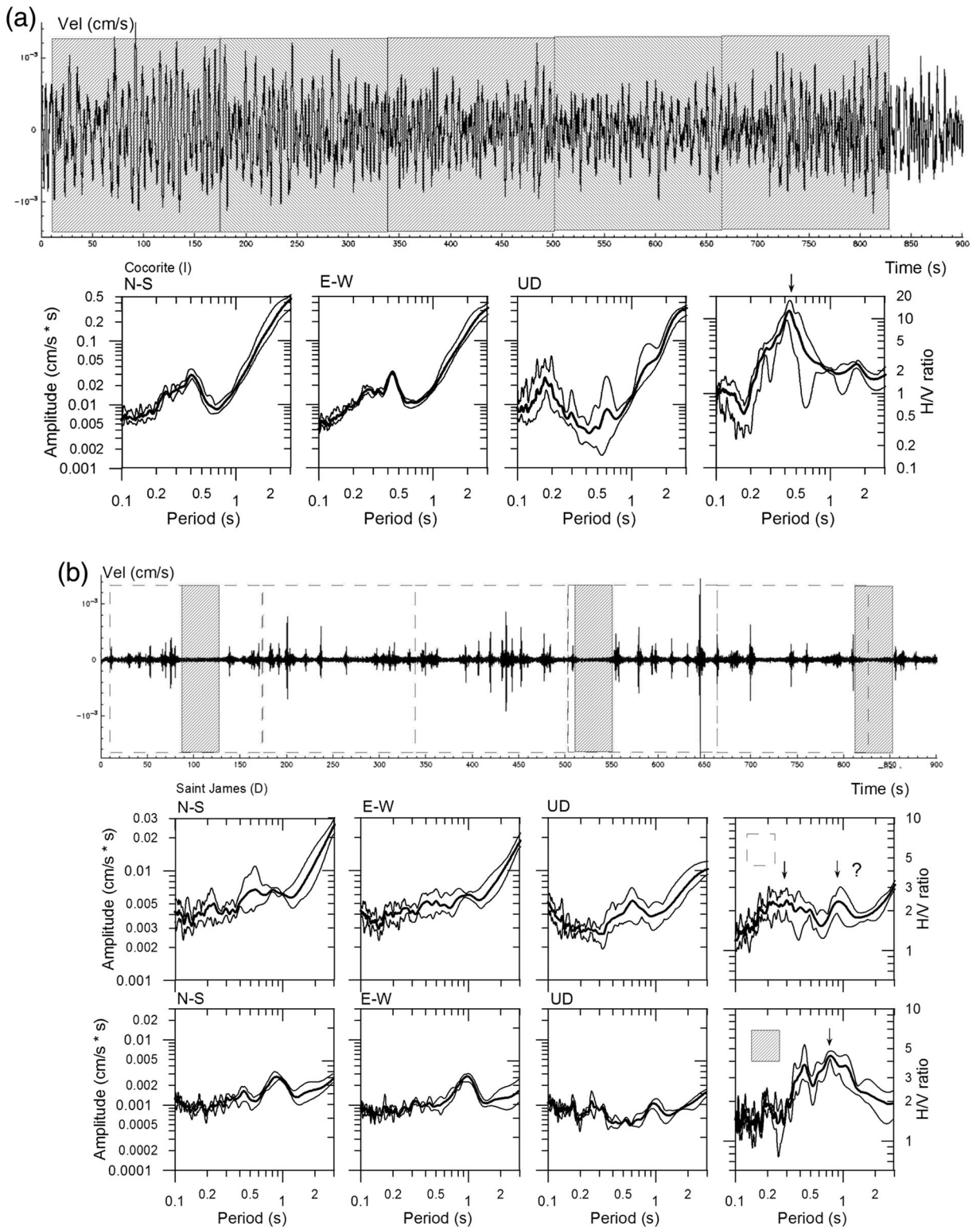
POS is the capital city of Trinidad and Tobago in the Eastern Caribbean (Fig. 1a), and it lies on an alluvial fan deposit caused by three main rivers that flow from the north through the city and its environs, namely, the Maraval River (west), the St. Ann’s River (north-east), and the Cascade River (north). This alluvium forms Port of Spain’s coastal aquifer and comprises Quaternary gravel beds such as the Port of Spain gravels (Fig. 1b; Barr and Saunders 1965). The Port of Spain gravels consist of poorly sorted gravels, sand, clay, and boulders. The part of today’s downtown Port of Spain closest to the sea was once an area

of tidal mudflats covered by mangroves. Toward the coast, the once mangrove swamps of the area have been reclaimed by anthropological means with a high water table. The fan rises gently from sea level in the port of Port of Spain to above 30 m elevation to the north where it meets the foothills of the Northern Range which is composed of Chancellor schist. The Cretaceous Lavantille Metalimestone Hills dominates East Port of Spain and it is comprised of massive, hard, gray fossiliferous limestones and black slates. Few wells dug into the alluvium have reached the bedrock and thus the fundamental period of vibration, the depth of the sediments, and the corresponding shear wave velocity are not well known in a wide area of the city. A recent probabilistic seismic hazard in the region (Bozzoni et al. 2011) suggested a peak ground acceleration of about 0.6 *g* on rock sites for a 2475-year return period in Port of Spain due to the influence of subduction zones, strike slip, and normal nearby faults. Details of the tectonics around Trinidad and the Eastern Caribbean can be found in Salazar et al. (2013a).

3 Methods and data

3.1 High-resolution mobile microtremors survey and predominant period of vibration of soil deposits

We performed a mobile microtremors survey from June 2013 to March 2014 in 16 areas (A–P in Fig. 1b) in POS. A total of 1181 measurements with an average of 85 m spacing were made employing a triaxial Tokyo Sokushin 24-bit sensor, model VSE-15D6 with a flat response between 0.1 and 100 Hz and a recording system of $\Delta_t = 0.01$ s (100 samples per second); the sensors measured micromotion in terms of velocity. In general, measurements were done in environments with low ambient noise, for 15 min at each location; the horizontal sensors were located with north-south and east-west orientations (magnetic north); the geographical coordinates of each microtremor measurement were acquired by a GPS unit. Measurements in the downtown area were carried out on Sundays, between the hours of 4:00 a.m. to 11:00 a.m., and on heavily trafficked streets, from 4:30 a.m. to 6:00 a.m. Residential areas were usually measured on working days from 9:00 a.m. to 4:00 p.m. The survey thus far has been divided into 16 areas (A–P) as shown in Fig. 1b including the



◀ **Fig. 2** **a** *Top*: microtremor recording in Cocorite (area I) depicting the time window employed in the digital signal processing scheme (*dashed area* corresponding to 163.84 s each); *bottom*: Fourier amplitude spectra for the three components of motion (*N-S* north-south, *E-W* east-west, *UD* vertical) and the horizontal to vertical spectral ratio (*H/V*). **b** *Top*: microtremor recording in Saint James (area D) depicting the time window employed in the digital signal processing scheme, *open squares* corresponding to 163.84 s and *dashed squares* corresponding to 40.96 s; *middle*: Fourier amplitude spectra for the three component of motion (*N-S* north-south, *E-W* east-west, *UD* vertical) and the horizontal to vertical spectral ratio (*H/V*) for 163.84 s windowing; *bottom*: Fourier amplitude spectra and *H/V* ratios for 40.96 s windowing. Note that the clear predominant peak appears (*arrow*) for the shorter time window selection when the passing of the cars is excluded in the analysis. The mean amplitude is depicted with a *thick line*, while the maximum and minimum amplitudes are depicted by the *thin lines*. The predominant peak is indicated by the *arrows* in the *H/V* spectral ratios (*right bottom*)

peripheries of the city. The data was stored in a SAMTAC 802-H 24-bit recorder.

We tried to make the measurement whenever possible, in a silent environment for 15 min at each location

(trying to maintain the survey interval; however, there are some locations where we had to collect in the closest possible location relative to this interval), since the instrument can easily record surrounding noise such as heavy traffic or the eventual pass of pedestrians near the sensors. These are reflected as spikes on the records that can perturb the periodic features of the microtremors. To avoid padding with zeros, the signal employing the fast Fourier transformation (FFT), samples of 163.84 s (which the number of velocity values matches the power of two = 2^{14} in accordance with the recording rate of 100 samples per second) of the stationary parts of the recording were selected initially for processing (see Fig. 2a). However, under some circumstances, we could only perform the measurements when constant pass of vehicles was inevitable at the site (e.g., roads or highways that have traffic 24 h a day); in these cases, we retrieved from the records shorter stationary parts of 40.96 s that also matches the power of two = 2^{12} (Fig. 2b). The first 10 s of the recordings were not selected for the analysis because we would usually close the cover of the

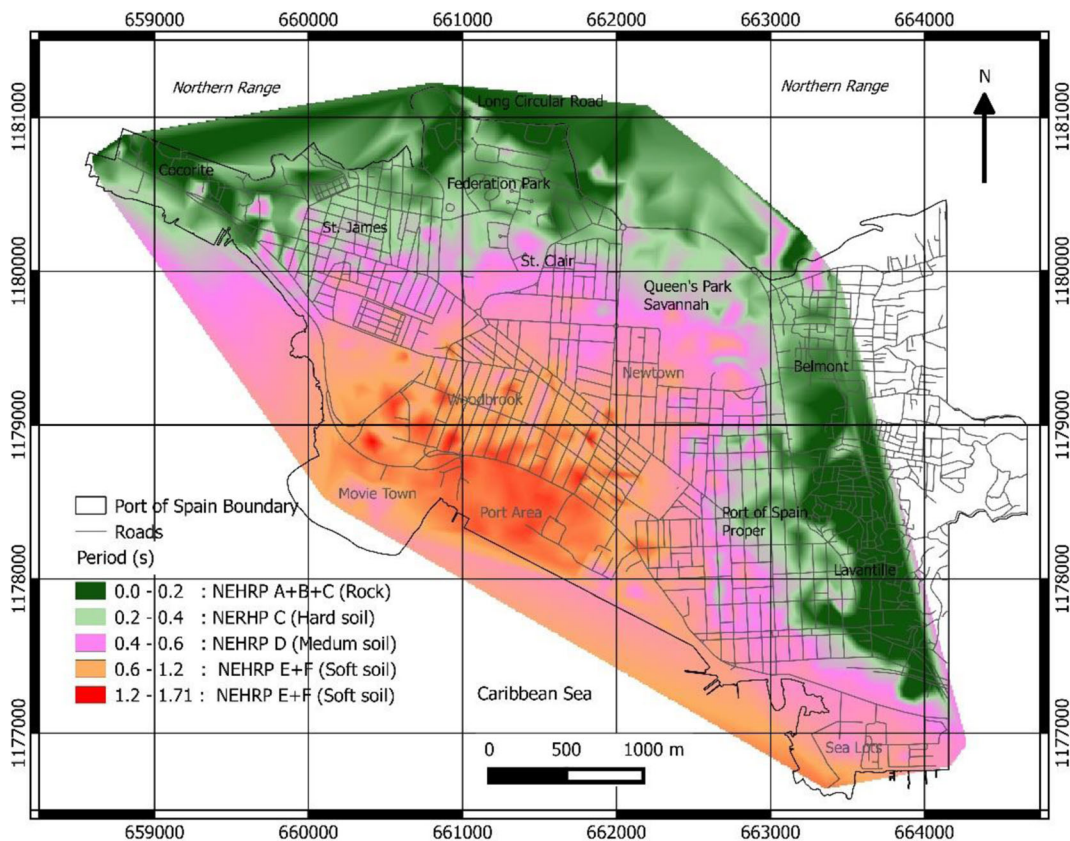


Fig. 3 Isoperiod map for Port of Spain. We divide the survey area into different zones according to its corresponding fundamental period *T* (s) of soil deposits based on NEHRP and Zhao and Xu (2013) soil classes

Table 1 Site class definitions (after Zhao and Xu 2013)

| Site class | Description | Natural period of soil | V_{s30} calculated from site period | NEHRP site classes |
|------------|-------------|--|--|--------------------|
| SC I | Rock | $T < 0.2$ s | $V_{s30} > 600$ m/s | A + B + C |
| SC II | Hard soil | $0.2 \leq$ (less or equal) $T < 0.4$ s | $300 < V_{s30} \leq$ (less or equal) 600 m/s | C |
| SC III | Medium soil | $0.4 \leq$ (less or equal) $T < 0.6$ s | $200 < V_{s30} \leq$ (less or equal) 300 m/s | D |
| SC IV | Soft soil | $T \geq 0.6$ s | $V_{s30} \leq 200$ m/s | E + F |

V_{s30} average shear wave velocity in the first 30 m

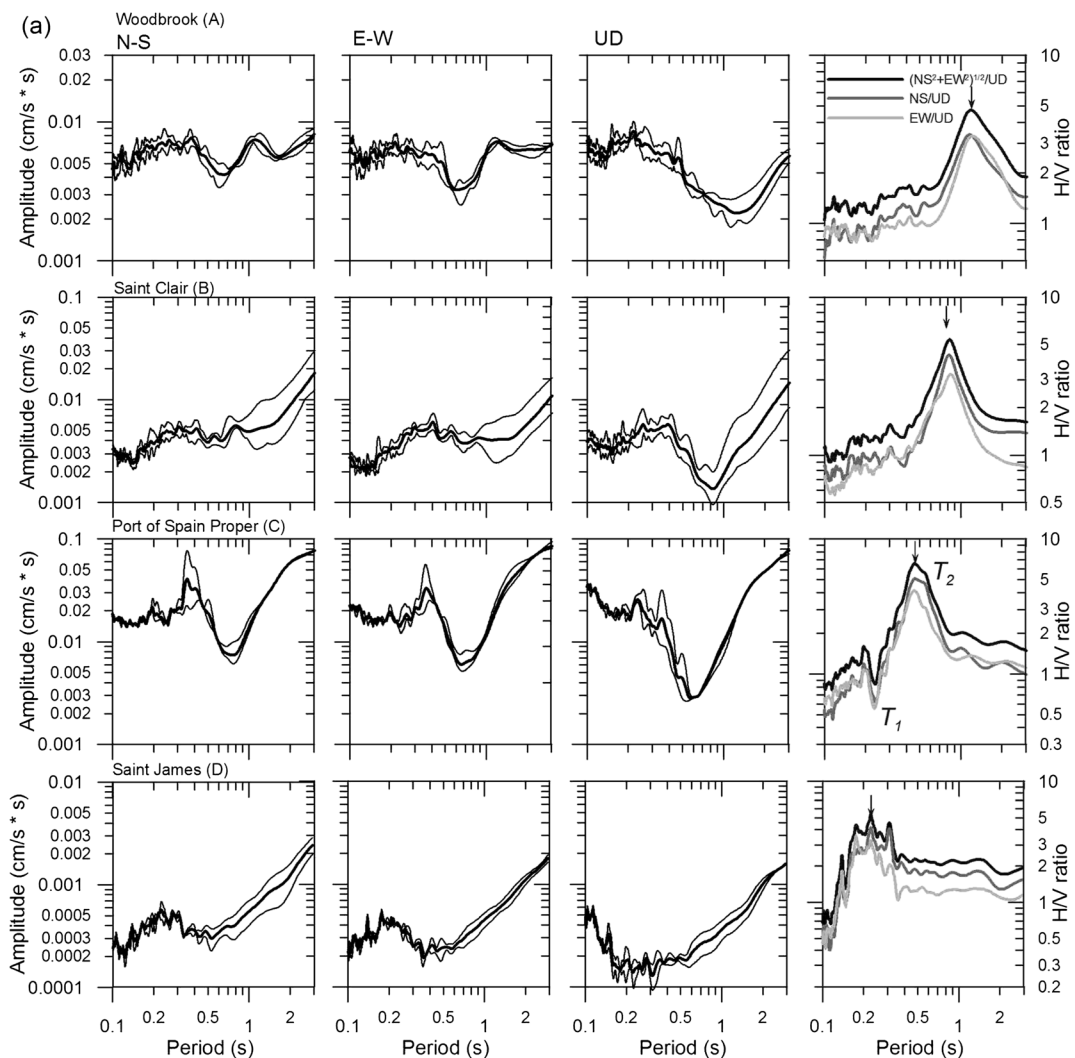


Fig. 4 Absolute Fourier amplitude spectra for velocity (*thick line*: mean, *thin line*: maximum and minimum) and H/V spectral ratios at 16 sites in different areas of Port of Spain. **a** Areas A–D; **b** areas E to H; **c** areas I to L; **d** areas M–P in Fig. 1b. The H/V ratios are computed using the resultant vector of the orthogonal north-south and east-west components of motion and averaging the results for all the stationary parts selected for each record. T_1 is nearly $1/2T_2$ indicating a high contrast between the sediments and the basement rock. Fundamental period of vibrations is indicated by the *arrows* in the H/V spectral ratios (*right*)

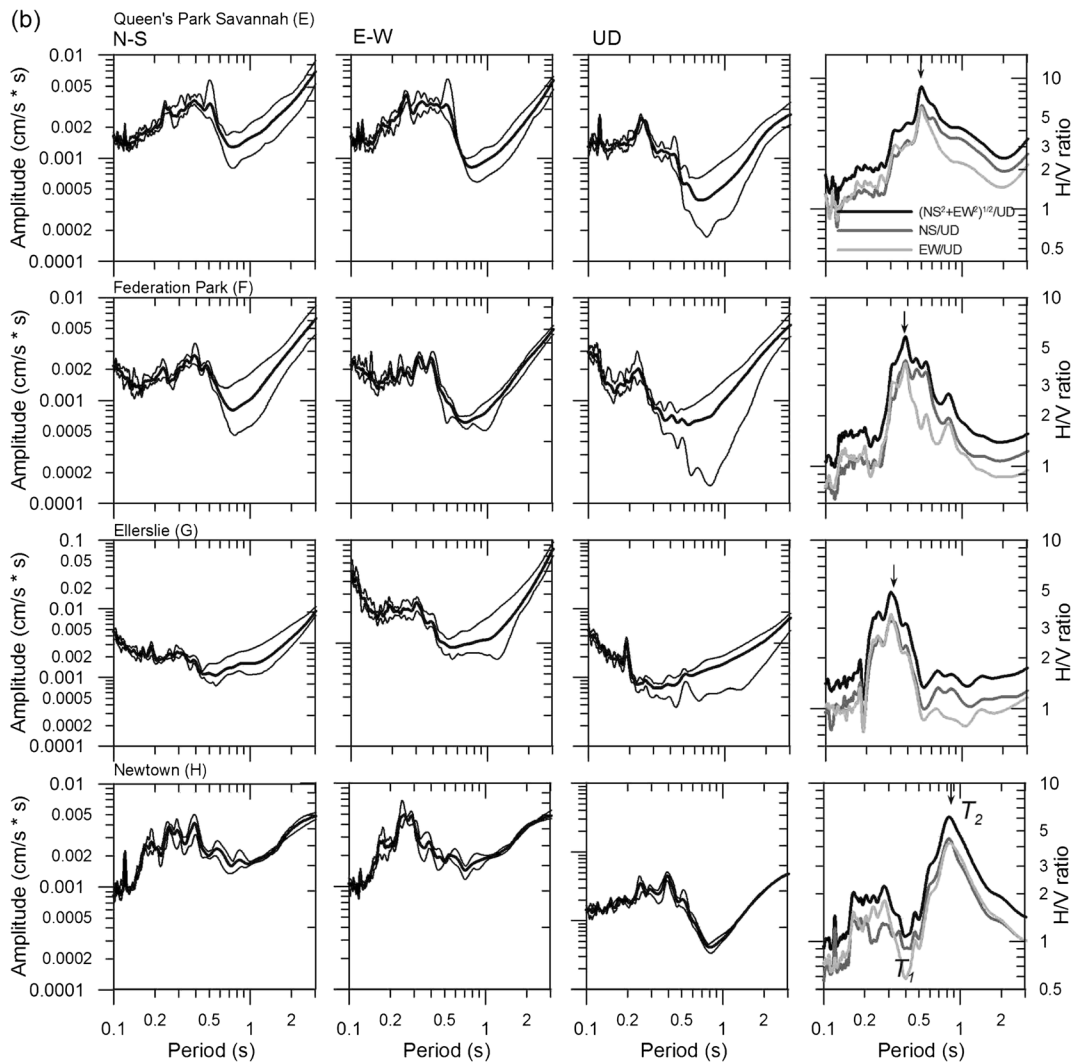


Fig. 4 (continued)

recorder and walk next to the instrument which results in spikes that would affect the stationary characteristics of microtremors.

We selected the low cutoff frequency in the filter according to the dynamic amplification factor (flat response) provided by the sensor manufacturer and the high cutoff frequency as $1/2\Delta_t = 50$ Hz, which corresponds to the Nyquist frequency physically representing the maximum frequency to be analyzed in discrete functions. For each corrected stationary part, we computed the resultant Fourier velocity amplitude spectrum and computed the mean of all parts and the corresponding uncertainties for the horizontal

and vertical components of motion. In this case, the uncertainty was computed in terms of the minimum and maximum spectral velocity observed during the measurements. We smoothed the spectra applying a Parzen window with a bandwidth of 0.3 Hz (Salazar et al. 2013b). Finally, after verifying the similarity in both horizontal components, we calculated the horizontal to vertical spectral ratio (H/V) employing the resultant vector of the orthogonal north-south and east-west components of motion. We identified the peak in the Nakamura H/V ratio (the predominant period) and located it in the geographical information system. We plotted the spectra for 0.1 to 3.0 s

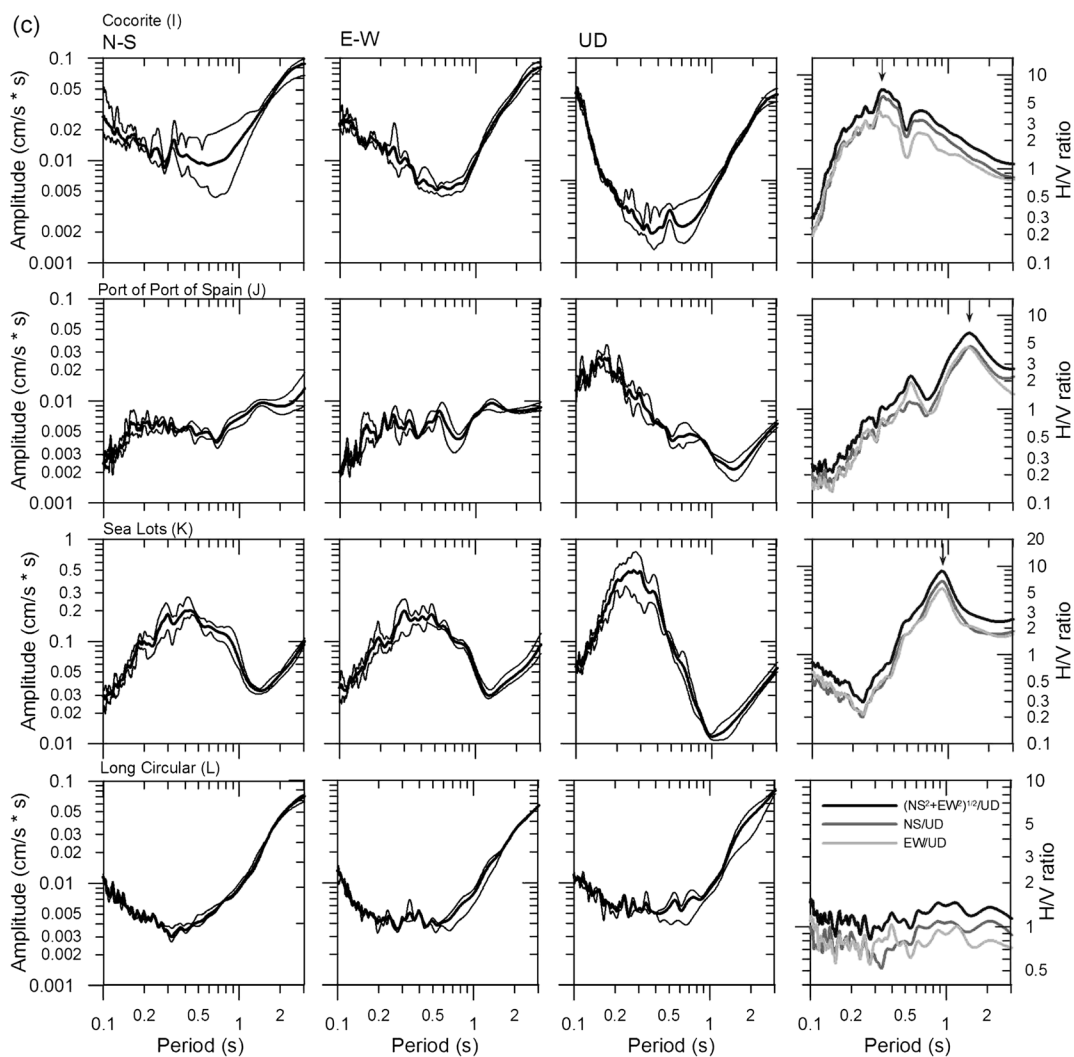


Fig. 4 (continued)

coinciding with the period range of interest for engineering practice (Fig. 2).

We plotted the resulting predominant periods of vibration of the soil for the 1181 microtremor points at each point of measurement over the geological classification map (Fig. 1b), and we developed a map with isoperiod patches corresponding to a grid of $10\text{ m} \times 10\text{ m}$ via application of the linear triangular interpolation method (Fig. 3). The isoperiod map is developed adopting the soil classes proposed by Zhao and Xu (2013) based on Building Seismic Safety Council (2000) NEHRP guidelines (Table 1). The longest periods of vibration in POS appear east of

the port area, movie town, and the south part of Saint James; it is between 1.2 and 1.7 s resulting from both deep sediments and reclaimed land. The area of Sea Lots results in predominant periods between 0.9 and 1.2 s on a swampy area. Periods between 0.6 and 0.9 s are observed in Newtown, and intermediate periods (0.3–0.6 s) are observed in the Queen's Park Savannah, Port of Spain Proper, Federation Park, Saint Clair, and the North Part of Saint James on recent alluvium. The shorter period yields less than 0.3 s in the peripheries of POS, Long Circular and Belmont, and east of POS, corresponding to a very stiff soil condition with very clear rock formation in the

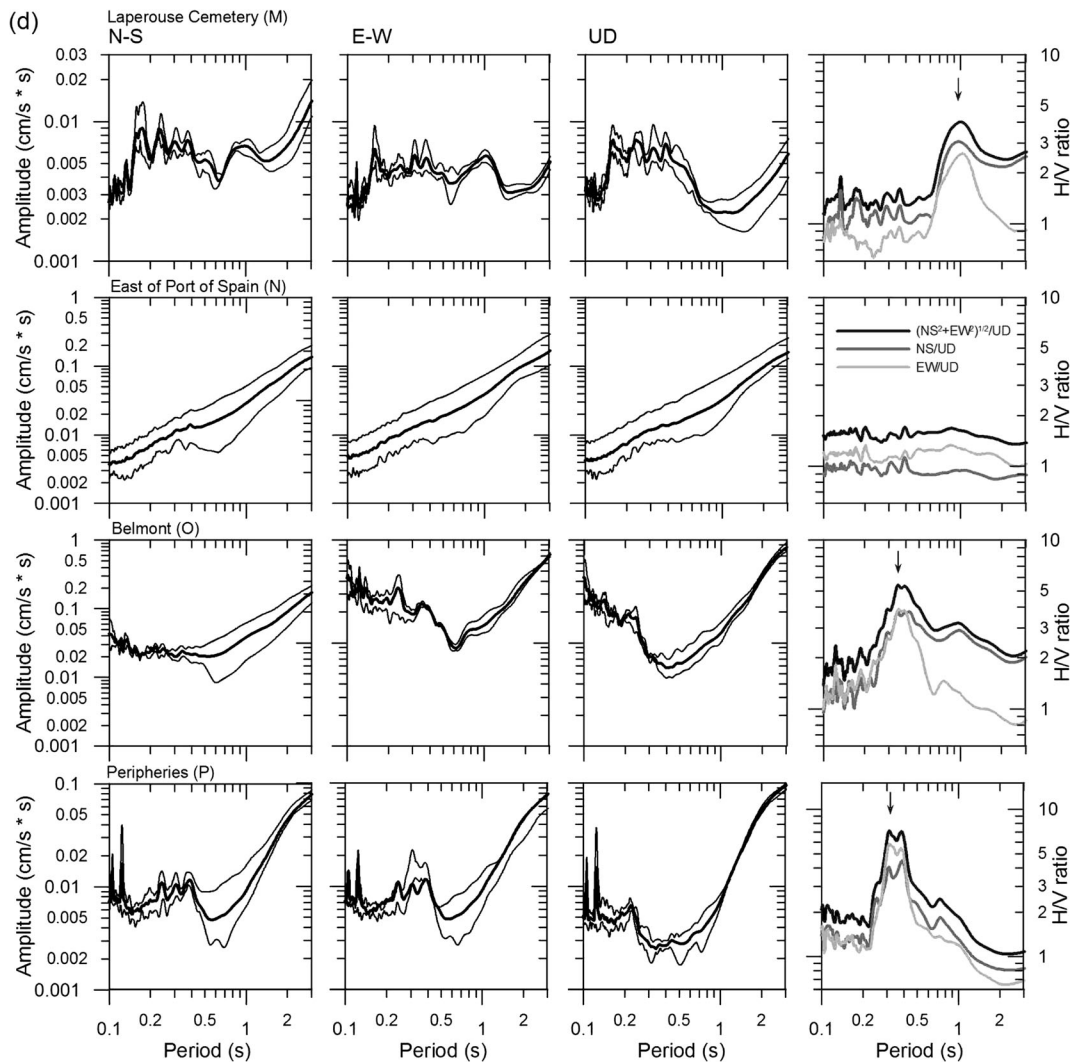


Fig. 4 (continued)

Lavantille area of Cretaceous Limestone, which is in accordance with the mapped geological conditions.

4 Results and discussion

4.1 Features of H/V spectral ratios

Our high-resolution survey deserves the presentation of the shape of the H/V spectral ratios and the absolute velocity Fourier amplitude spectra; we plot them for one site of each of the 16 areas in the city of POS. The shape of the H/V ratios and spectra introduces an insight to the wave propagation of microtremors in Port of Spain (Fig.

4a–d): an important characteristic of this transfer function is that the peak observed in H/V ratios of vibration is clearly caused by the trough in the vertical component physically representing the change from prograde to retrograde particle motion at the surface; in other words, the ellipticity of the fundamental modes of Rayleigh waves explains such peak at the first mode of vibration (Bonnetoy-Claudet et al. 2006).

In some cases, note that the trough period T_1 is nearly half of the peak period T_2 in the H/V spectral ratios presented in areas as Port of Spain Proper (area C, Fig. 4a) and Newtown (area H, Fig. 4b). Previous studies have demonstrated that the sharp peak (T_2) and a sharp trough (T_1) suggest a high

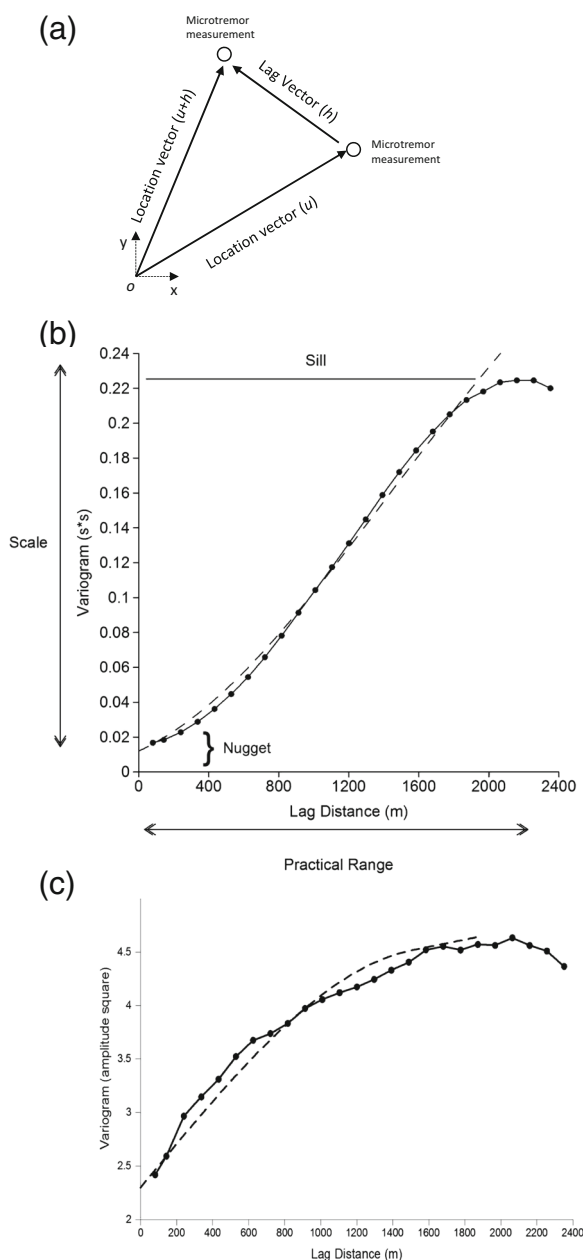


Fig. 5 **a** Illustration of lag distance or vector h between two microtremor points employed to construct an experimental variogram. **b** Omnidirectional experimental variogram for the fundamental period of vibration depicting the spatial variability with distance (solid line with dots). **c** Omnidirectional variogram for the peak ratios with distance. Broken line: Gaussian and circular model for the period and the peak ratio, respectively. Settings for Gaussian model: 0.2 s^2 for the scale, 2000 m for the practical range and 0.012 s^2 for the nugget effect. Setting for the circular model: 1.7 amplitude square for the scale, 1500 m for the practical range, and 2.3 amplitude square for the nugget effect

velocity contrast (high impedance) between the basement rock (V_R) and the velocity of the surface layers (V_S) yielding $V_R/V_S \geq 2.5$ (Konno and Ohmachi 1998). The shear wave velocity V_R west of Trinidad at the North Eastern Venezuela is reported by Schmitz et al. (2005) equal to $V_R \approx 2000 \text{ m/s}$; the average shear wave velocity V_S for the soil deposits in Port of Spain Proper (Woodford Park site) according to preliminary genetic inversion on phase velocity of microtremors array yields $V_S = 446 \text{ m/s}$; then, $V_R/V_S \approx 4.5 > 2.5$.

The shapes of the absolute spectra and the H/V ratios at Cocorite (Fig. 4c, zone I) yield different features in comparison with other parts of POS. It is noticed that the second mode of vibration of 0.32 s constitutes the predominant period, in this case with a first mode at 0.65 s suggesting intercalation of rigid and soft materials in this area; both peaks are caused again by the trough in the vertical component (Salazar and Seo 2002, Salazar et al. 2007).

Stiff soil conditions are found on the east part of Port of Spain (Lavantille, area N Fig. 4d) and Long Circular Road (Fig. 4c, area L), yielding an H/V ratio ≈ 1.0 for periods between 0.1 and 3.0 s representing a circular wave particle motion instead of an elliptical one. However, the usable frequency range of the microtremor sensors permitted analysis of periods from 0.02 s to 0.1 s (10 to 50 Hz —which is the Nyquist frequency); in such cases, we replot the ratios and revise carefully if a peak is located below 0.1 s . If we identified a clear peak, we set it as the fundamental period belonging to very shallow weathered layers at rock sites; otherwise, we set a zero value for the fundamental period and a value of one for the ratio (Fig. 4d, East Port of Spain).

We also plotted the H/V spectral ratio corresponding to the N-S and E-W direction separately (Fig. 4a–d), and we did not find a clear directivity effect (Matsushima et al. 2014) at this time since both components basically yield the same peak ratios.

4.2 Measure of spatial variability

Our dense mobile microtremor survey permits to have a measure of the spatial variability of fundamental periods and peak ratio with distance. We measured such variability via application of a variogram plot (Rorbach et al. 2008; Abid et al. 2015). For all possible locations u , the variogram

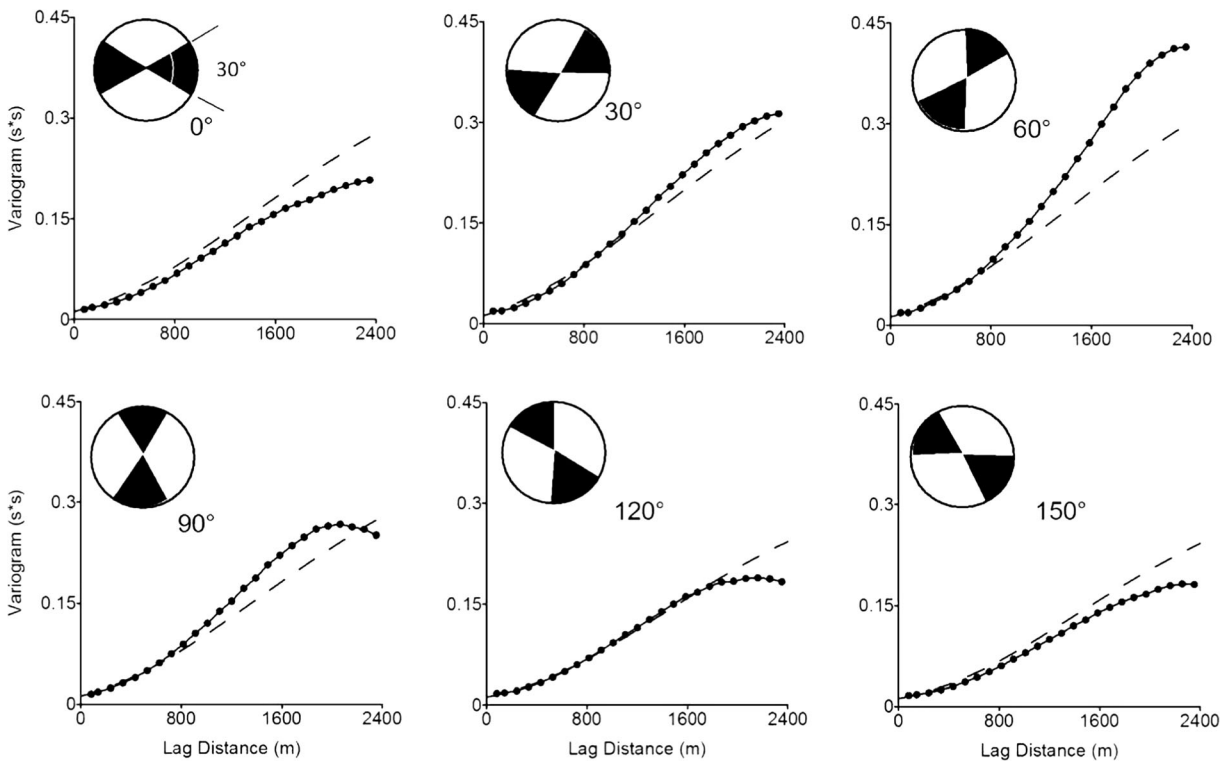


Fig. 6 Directional variogram plots for the period of vibration of soil deposits, with tolerance set to 30°. The circular diagrams depict both the tolerance and the

direction of the lag vector h . *Solid line with dots*: experimental data; *broken line*: Gaussian model for the omnidirectional case

for a lag distance h is defined as the average square difference of values separated approximately by h as:

$$2\gamma(h) = \frac{1}{N(h)} \sum_{N(h)} [Z(u) - Z(u + h)]^2 \quad (1)$$

$N(h)$ is the number of pairs for lag distance or vector h , and $Z(u)$ and $Z(u + h)$ are the values of the fundamental period or peak ratio at distances u and $u + h$, respectively (Fig. 5a). The experimental variograms are presented in Fig. 5b, c setting the lag width as 96 m, and the number of lags as 25 yielding a maximum lag distance of 2400 m. For short distances of about 100 m, the variogram plot yields a variability of 0.012 s^2 ($\approx 0.1 \text{ s}$) and 2.3 (amplitude square) for the all periods of motion and the peak ratio, respectively, which is related as the nugget effect. As expected, the variability increases with distance. While the variability of the period can be modeled as Gaussian distribution, the variability of the peak ratio

suggests a circular one. The Gaussian model can be written as follows:

$$g(h) = c \left(1 - \exp\left(\frac{-3h^2}{p^2}\right) \right) \quad (2)$$

where h represents the lag distance, p represents the practical range, and c is the sill (Fig. 5b), representing the value at which the variogram levels off and there is no more spatial correlation. The difference between the sill and the nugget is the scale.

The spherical model yields:

$$g(h) = c \left(1.5 \left(\frac{h}{p}\right) - 0.5 \left(\frac{h}{p}\right)^3 \right) \quad (3)$$

Note that Fig. 5b, c corresponds to omnidirectional variograms which average the behavior over all directions. We investigated the possibility of anisotropy, that is, the property of the lag distance h being directionally dependent (Budrikaitė and Dučinsas 2005). Thus, we developed experimental variograms setting the lag

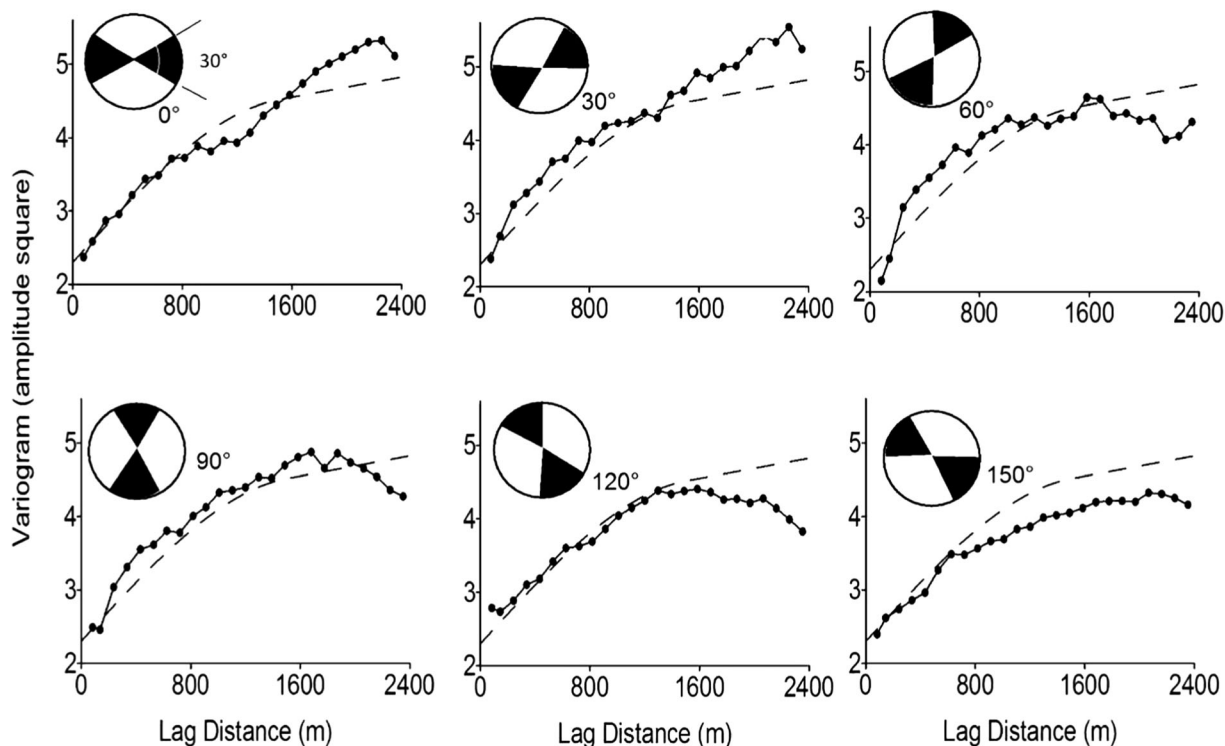


Fig. 7 Directional variogram plots for the peak ratio, with tolerance set to 30° . The circular diagrams depict both the tolerance and the direction of the lag vector h . *Solid line with dots*: experimental data; *broken line*: circular model for the omnidirectional case

direction from 0° to 150° with rotations anticlockwise every 30° with a tolerance of 30° , namely, the shadow area in the circles depicted in Fig. 6; then, the microtremors considered in the variogram plot for each case belong only to the data that lay inside into the angular tolerance. Note that the lag direction for 0° is equal to 180° . The results are presented in Fig. 6 for the period and Fig. 7 for the peak ratio or amplitude. In terms of period, for all directions, the omnidirectional model is consistently only to the left of the ascending portion of the experimental variograms and the scale changes from 0.16 to 0.40 s^2 . The maximum scale is obtained for 60° , so the minimum scale that corresponds to a minimum variability might be located at the orthogonal direction of $150^\circ = 60 + 90$. This is an indication for geometric anisotropy.

We found implementing the Powell's search method (Press et al. 1992) that the best fit model to our period experimental data at the minimum variability yields when using the Gaussian distribution considering the effect of the geometrical anisotropy, that is, the property of the lag distance h being directionally dependent with an angle θ of 148° (anticlockwise from the east or x positive axis)

and a ratio $r = a/b$ of 1.6 (see Fig. 8a) and setting the scale as 0.18 s^2 , the practical range $p = 2200 \text{ m}$, and the nugget effect as 0.010 s^2 . We attribute the anisotropy represented in the angle θ and r to the prominent directionality in the depositional setting along and perpendicular to the main rivers in POS (Fig. 1b); indeed, such angle fairly coincides with the alignment of the coastline (30° clockwise from the horizontal). In other words, the value of the fundamental period changes more quickly along the longitudinal axis a of the ellipse depicted in Fig. 8a at a rate of 1.6 relative to the perpendicular axis b .

In terms of amplitude (Fig. 7), the scale changes from 1.3 to 3.0 with the minimum variability located at 150° . We found the angle $\theta = 139^\circ$ and ratio $r = 2.0$ to model the anisotropy of the peak ratio with a circular model and setting the scale as 1.3 amplitude square, the practical range as 1600 m , and a nugget effect of 2.3 amplitude square (Fig. 8b). These results are very important for the sake of future stochastic simulations or kriging processes employing microtremors. These results are then utilized to interpolate between the known data to find the missing data in order to define a complete zonation map of the spatial area of interest, then kriging is utilized when there

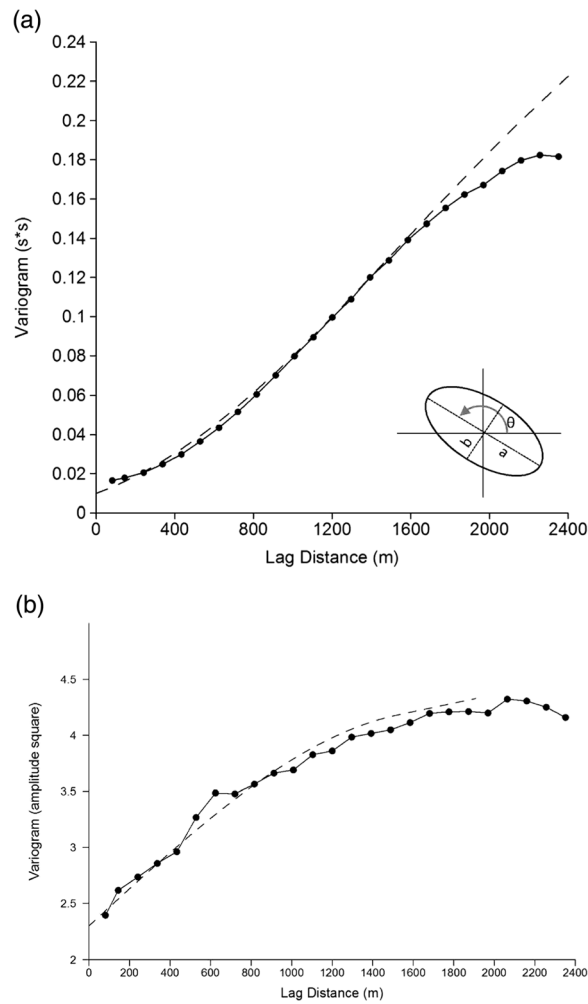


Fig. 8 Directional variograms and anisotropy. **a** Period of vibration of soil deposits; *solid line with dots*: experimental data; *broken line*: Gaussian model setting 0.18 s^2 for the scale, 2200 m for the practical range and 0.010 s^2 for the nugget effect, anisotropy ratio $r = a/b$ of 1.6 and angle θ of

148° . **b** Peak ratio; *solid line with dots*: experimental data; *broken line*: circular model setting 1.3 amplitude square for the scale, 1600 m for the practical range and 2.3 amplitude square for the nugget effect; anisotropy ratio $r = a/b$ of 2.0 and angle θ of 139°

is prohibitive cost or logistics in collecting actual observations when a second set of estimated observations can be used to fill in the data gaps in similar geological environments (Rorbach et al. 2008). For example, in order to expand the zonation in POS, the results can be extended toward the outskirts of the city of POS or apply them to other cities in Trinidad or at the Caribbean Islands with similar geomorphological conditions.

4.3 Comparison of microtremors and earthquake motion

During the survey in the district of Woodbrook, we recorded one small earthquake dated on July 11th,

2013, at 10:37 local time with a M 3.4, epicentral coordinates of 11.489 N, 62.183 W. and a depth of 20 km, located north of Paria Peninsula (North West Trinidad), approximately 150 km away from POS. We retrieved the S-wave part of the earthquake recording and computed the H/V ratio and compared with the ones of the microtremor (ambient noise)—see Fig. 9. A period of 1.0 s is observed for both the earthquake and the microtremor recordings even with the same level of amplification of 4–5. This exercise demonstrates that a strong motion network in POS might be an essential part of future research to understand more precisely the amplification characteristics of the soil in the area and

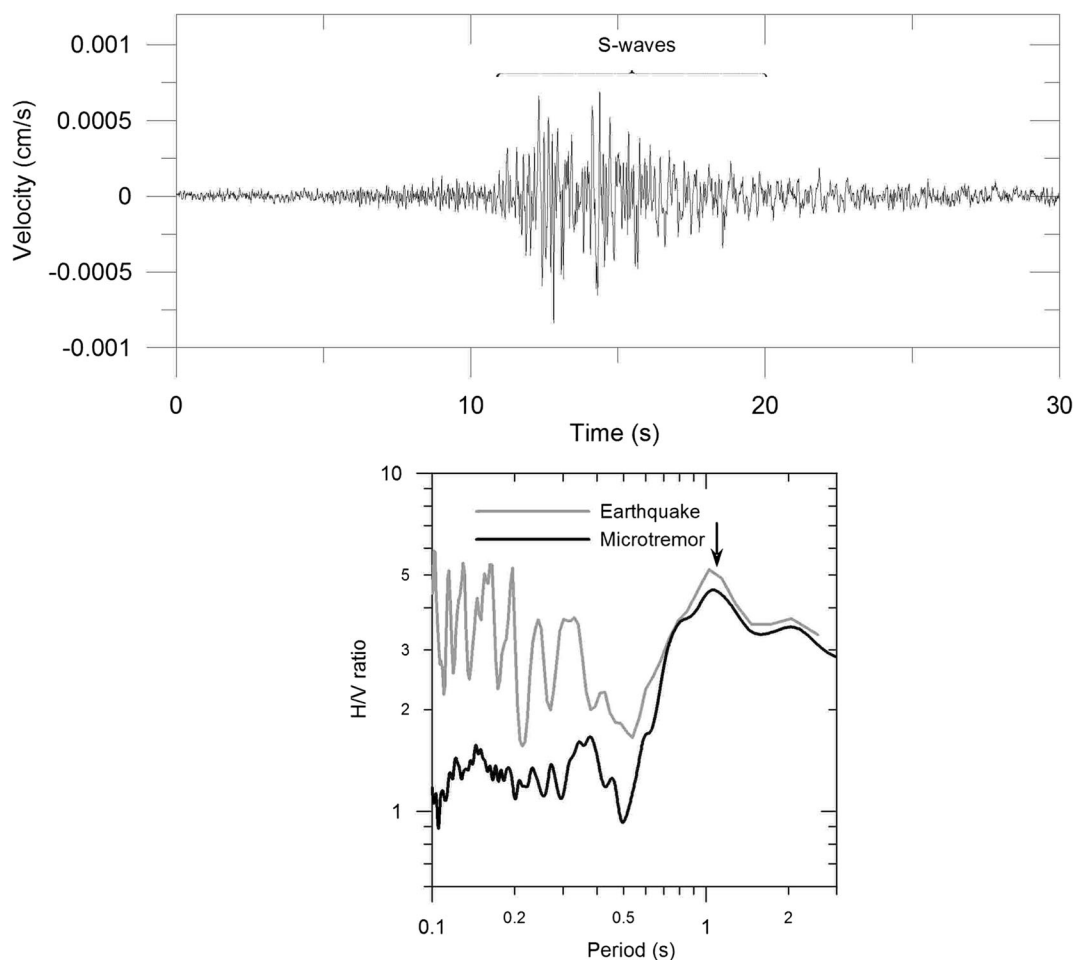


Fig. 9 Comparison of earthquake and microtremor measurement. *Top:* E-W component recorded on July 11, 2013, 14:37 UTC M 3.4 at 11.489 N, 62.183 W with depth of 20 km in Woodbrook area of POS during the microtremor survey. *Bottom:* Comparison of H/

V spectral ratios between earthquake data (S waves) and microtremors in Woodbrook area. Clear predominant peaks are indicated by the *arrows*

compare the results of the H/V spectral ratios employing microtremors.

4.4 Elastic design response spectra

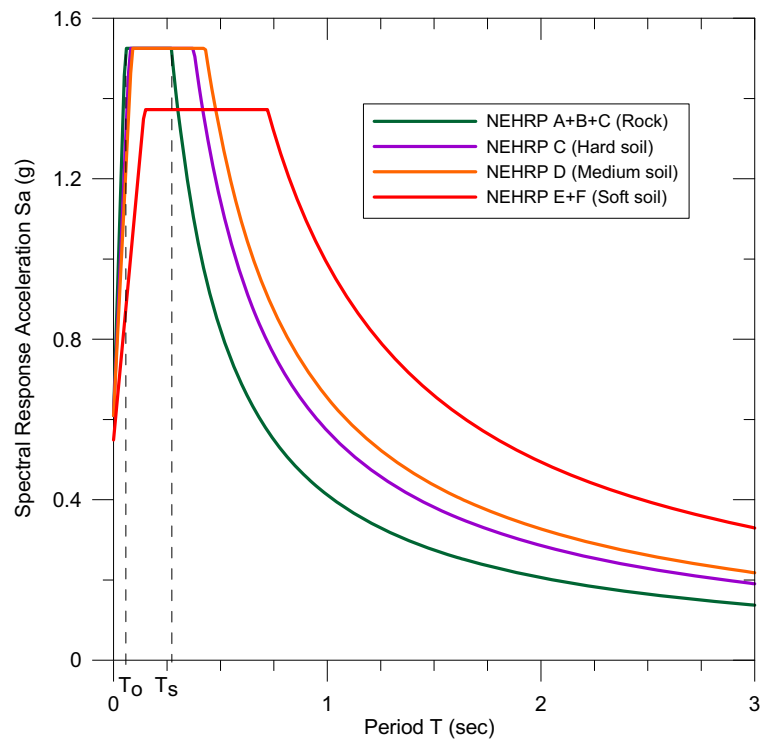
In this section, we propose preliminary elastic design response spectra of 5% damping for different soil classes at POS. We used the Zhao and Xu (2013) classification based on the soil period of vibration retrieved from the H/V spectral ratios on microtremors (see Table 1 and Fig. 3).

Bozzoni et al. (2011) developed probabilistic seismic hazard maps for rock sites (NEHRP site class B) assuming a flat topography in the Eastern Caribbean including Trinidad compatible with the International Building Code provisions (International Code Council (ICC)

2009). Then, we retrieved from the maps the acceleration spectral ordinates at 0.2 and 1.0 s in Port of Spain yielding 1.53 and 0.41 g, respectively, for 2500 years return period corresponding to 2% of probability of exceedance in a 50-year lifetime of the structure. The complete rock site response spectrum ranging from 0 to 3 s was developed using the ASCE 7-10 (2010)/IBC spectral shape formulation based on the short and long period acceleration spectral response above. The rock site spectrum was modified based on the site coefficients based on NEHRP soil classes in Port of Spain (Table 1). The results are presented in Fig. 10.

The elastic seismic design coefficients are characterized by the linear ascending acceleration trend for short period structures ranging from 0 s to period T_0 , by a

Fig. 10 Elastic design response spectra for 5% damping setting 2500 years return period for the zones depicted in Fig. 3 based on NEHRP and Zhao and Xu (2013) soil classes



constant value at intermediate periods from T_0 to the transition period T_s and later by an exponential decay after T_s toward long period components (Fig. 10). It is noted that amplification takes place after the transition period T_s in soil classes C and D in the order of 1.3 to 1.6 times the spectral acceleration on rock sites. However, a deamplification is observed for soil class E + F in the short period components and an amplification factor of 2.4 is proposed for longer period components. Note that when applying the ASCE 7-10 spectral shape formulation, the transition periods T_s yielded 0.38, 0.43, and 0.75 s for soil classes C, D, and E + F, respectively, which lay inside the period range proposed by Zhao and Xu (2013).

In order to validate such amplification features in POS disposed by NEHRP guidelines, linear and nonlinear transfer functions must be derived retrieving the shear wave velocity profiles at several sites in the city; as a first step, nine microtremor array measurements were done in different parts that are actually under investigation via application of phase velocity inversion and the diffuse field approach. These geophysical prospecting results might also be correlated with borehole available data to complete a seismic microzonation study, and it would help to differentiate the rock site (NEHRP A + B + C) and soft soil (NEHRP E + F) classifications used in this study.

4.5 Conclusions

We performed a dense mobile microtremor survey with an average spacing of 85 m which permitted us to retrieve the fundamental period of soil deposits for POS and proposed a preliminary elastic design response spectrum for 5% damping.

We have proposed a map in terms of fundamental period of soil deposits for POS measuring the variability of period and peak ratio with distance through variogram plots, incorporating the anisotropy in the Gaussian and circular models to be used in future stochastic simulations. Then, we have divided the city into four zones according to period of vibration that can be used for planning purposes based on the design response spectra (Figs. 3 and 10), e.g., retrofit activities for some buildings and residential houses or to avoid the construction of new buildings that could experience the resonance phenomena when both the period of the soil and the period of the structure coincide when the next earthquake strikes. Small irregularities and the variability in the isoperiod patches might be related to the heterogeneous quality of landfill activities for building foundation works in POS. Very stiff site conditions are clearly found in the east part of POS in the Lavantille hilly area; ironically, this area is being considered the most dangerous due to the high rates of crime and the lowest

income level in POS, while important industry facilities are located on the soft and thicker sediments.

A high-resolution digital elevation model must be developed in order to produce detailed slope maps for POS and consequently V_{s30} estimations to correlate with the periods of soil deposits obtained in this study (Allen and Wald 2007, 2009; Wald and Allen 2007). However, we suggest to characterize the soil profiles by the fundamental period of vibration rather than the V_{s30} for POS (McVerry 2011). Zhao and Xu (2013) suggest also that site period is a better parameter for characterizing soil conditions in very deep or very soft sediments.

The source of the microtremors can be elucidated if continuous measurements during day- and nighttime at different seasons are performed simultaneously on rock and soil and compare their amplitude with those of ocean wave heights or changes in atmospheric pressure with proper instrumentation in the port area. Then, the long period microtremors (microseisms) and short period microtremors (Kanai's microtremors) must be distinguished in future research with continuous measurements at strategic points in the city at rock site and deep soil conditions.

The installation of a new strong motion network in POS is a must for future earthquake engineering research in Trinidad as we demonstrated in Fig. 9, when comparing the H/V ratios of microtremor and the earthquake shaking. The authors recommend installing at least one instrument at the rock in Lavantille area which will be the reference rock site and at least five strong motion instruments per zone depicted in the isoperiod map. This would allow conducting two additional techniques, namely a generalized inversion analysis on strong motion data and the traditional spectral ratios (soil/rock site) to retrieve the transfer function of the soil (see Salazar et al. 2007) and compare with the amplification factors that results from the microtremors. The last hazard maps for Trinidad have been proposed by Bozzoni et al. (2011) yielding 0.60 g of peak ground acceleration and 1.53 and 0.41 g spectral acceleration for 0.2 and 1.0 s, respectively, for POS setting 2500 years return period at a rock site; this shaking level will be amplified according to the findings of this work causing severe damage at the typical constructions in the city.

Future risk maps will be possible at POS if a vulnerability assessment and socioeconomic research is well conducted with the corresponding new probabilistic seismic hazard assessment for Trinidad incorporating

the effect of the Central Range Fault and the effects of soil amplification found in this work.

Acknowledgements The microtremor recordings were provided by the Ministry of Planning and Sustainable Development of Trinidad and Tobago and are proprietary.

We used QGIS Open Software version 2.4 to generate the maps presented in this work and the GCC Fortran Compiler. The mobile microtremor survey was basically done by only two persons, the first author and one of the co-authors during a whole year, and we thank God for giving us the necessary strength to finalize this work.

References

- Abid A, Afzal P, Heydarzadeh K (2015) Site effect classification on microtremor data using a concentration-area fractal model. *Nonlin Processes Geophys* 22:53–63
- Allen, T., and D. Wald (2007) Topographic slope as a proxy for seismic site-conditions (V_{s30}) and amplification around the globe. *Open-File Report 2007–1357*. U.S. Geological Survey, Reston, Virginia
- Allen T, Wald D (2009) On the use of high-resolution topographic data as proxy for seismic site conditions (V_{s30}). *Bull Seismol Soc Am* 99(2A):935–943
- ASCE 7-10 (2010) Minimum design loads for buildings and other structures. American Society of Civil Engineers. p. 658
- Barr, K. W., and J.B. Saunders (1965) An outline of the geology of Trinidad, *Notes from the Transactions of the Fourth Caribbean Geological Conference*, 7. Port of Spain: The University of the West Indies
- Bonnefoy-Claudet S, Cornou C, Bard P, Cotton F, Moczo P, Kristek J, Fäh D (2006) H/V ratio: a tool for site effects evaluation. Results from 1-D noise simulations. *Geophys J Int* 167:827–837
- Bozzoni F, Corigliano M, Lai C, Salazar W, Scandella L, Zuccolo E, Latchman J, Lynch L, Robertson R (2011) Probabilistic seismic hazard assessment at the Eastern Caribbean Islands. *Bull Seismol Soc Am* 101(5):2499–2521
- Budrikaitė, L. & K. Dučinsas (2005) Modelling of geometric anisotropic spatial variation. Mathematical modelling and analysis. Proceeding of the 10th International Conference MMA2005 & CMAM2, Trakai. 361–366
- Building Seismic Safety Council (2000) The 2000 NEHRP recommended provisions for new buildings and other structures: part I (provisions) and part II (commentary), FEMA 368/369. Federal Emergency Management Agency, Washington, D.C.
- International Code Council (ICC) (2009) 2009 ICC international building code, International Code Council, Inc., <https://www.iccsafe.org/>
- Konno K, Ohmachi T (1998) Ground-motion characteristics estimated from spectral ratio between horizontal and vertical components of microtremors. *Bull Seismol Soc Am* 88: 228–241
- Matsushima S, Hirokawa T, De Martin F, Kawase H, Sánchez-Sesma F (2014) The effect of lateral heterogeneity on

- horizontal-to-vertical spectral ratio of microtremors inferred from observation and synthetics. *Bull Seismol Soc Am* 104: 381–393
- McVerry, G. (2011) Site-effect as continuous functions of site period and V_{s30} . Proceedings of the ninth Pacific conference on earthquake engineering, building and earthquake—Resilient Society. 14–16 April, Auckland, New Zealand
- Nakamura Y (1989) A method for dynamic characteristics estimation of subsurface using microtremor on the ground surface. *Quick Rep Railw Res Inst* 30(1):25–33
- Press, W., S. Teukolsky, W. Vetterling & B. Flannery (1992) *Numerical recipes in Fortran 77: the art of scientific computing*. Second edition. Cambridge University Press. pp.933
- Rorbach, E., L. Liu, Q. Chen & W. Wang (2008) Borehole and microtremor data fusion for sediment layer thickness estimation in Beijing area. The 14th conference on earthquake engineering. October 12–17, Beijing, China
- Salazar, W. and K. Seo (2002) Spectral and amplification characteristics in San Salvador City (El Salvador) for upper-crustal and subduction earthquakes. *11th Japan Earthquake Engineering Symposium*, P065, pp. 329–334
- Salazar W, Seo K (2003) Earthquake disasters of January 13th and February 13th 2001, El Salvador. *Seismol Res Lett* 74(4): 420–439
- Salazar W, Sardina V, Cortina J (2007) A hybrid inversion technique for the evaluation of source, path and site effects employing S-wave spectra for subduction and upper-crustal earthquakes in El Salvador. *Bull Seismol Soc Am* 97(1B): 208–221
- Salazar, W., L. Brown and G. Mannette (2013a) Probabilistic seismic hazard assessment for Bridgetown-Barbados, employing subduction interface characteristic earthquakes. *J Civil Eng Archit*, volume 7, No. 11 (Serial No 72), pp. 1405–1422
- Salazar, W., L. Brown and G. Mannette (2013b) Surface soil effects studies based on H/V ratios of microtremors at Kingston Metropolitan Area, Jamaica. *J Civil Eng Archit*, volume 7, No. 10 (Serial No. 71), pp. 1301–1322
- Schmitz M, Alvarado L, & Lüth S (2005) The velocity structure of the Cariaco sedimentary basin, northeastern Venezuela, from the refraction seismic data and possible relation to earthquake hazard. *J South Am Sci* 18(2):89–105
- Wald D, Allen T (2007) Topographic slope as a proxy for seismic site conditions and amplification. *Bull Seism Soc Am* 97(5): 1379–1395
- Zhao J, Xu H (2013) A comparison of V_{S30} and site period as site-effect parameters in response spectral ground-motion prediction equation. *Bull Seismol Soc Am* 103:1–18